


RESEARCH

Open Access



Risk stratification of cardiac metastases using late gadolinium enhancement cardiovascular magnetic resonance: prognostic impact of hypo-enhancement evidenced tumor avascularity

Angel T. Chan^{1,2,3*}, William Dinsfriend¹, Jiwon Kim⁴, Brian Yum¹, Razia Sultana⁴, Christopher A. Klebanoff¹, Andrew Plodkowski², Rocio Perez Johnston², Michelle S. Ginsberg², Jennifer Liu¹, Raymond J. Kim⁵, Richard Steingart¹ and Jonathan W. Weinsaft^{1,2,4*} 

Abstract

Background: Late gadolinium enhancement (LGE) cardiovascular magnetic resonance (CMR) is widely used to identify cardiac neoplasms, for which diagnosis is predicated on enhancement stemming from lesion vascularity: Impact of contrast-enhancement pattern on clinical outcomes is unknown. The objective of this study was to determine whether cardiac metastasis (C_{MET}) enhancement pattern on LGE-CMR impacts prognosis, with focus on heterogeneous lesion enhancement as a marker of tumor avascularity.

Methods: Advanced (stage IV) systemic cancer patients with and without C_{MET} matched (1:1) by cancer etiology underwent a standardized CMR protocol. C_{MET} was identified via established LGE-CMR criteria based on lesion enhancement; enhancement pattern was further classified as heterogeneous (enhancing and non-enhancing components) or diffuse and assessed via quantitative (contrast-to-noise ratio (CNR); signal-to-noise ratio (SNR)) analyses. Embolic events and mortality were tested in relation to lesion location and contrast-enhancement pattern.

Results: 224 patients were studied, including 112 patients with C_{MET} and unaffected (C_{MET}^-) controls matched for systemic cancer etiology/stage. C_{MET} enhancement pattern varied (53% heterogeneous, 47% diffuse). Quantitative analyses were consistent with lesion classification; CNR was higher and SNR lower in heterogeneously enhancing C_{MET} ($p < 0.001$)—paralleled by larger size based on linear dimensions ($p < 0.05$). Contrast-enhancement pattern did not vary based on lesion location ($p = NS$). Embolic events were similar between patients with diffuse and heterogeneous lesions ($p = NS$) but varied by location: Patients with right-sided lesions had threefold more pulmonary emboli (20% vs. 6%, $p = 0.02$); those with left-sided lesions had lower rates equivalent to controls (4% vs. 5%, $p = 1.00$). Mortality was higher among patients with C_{MET} (hazard ratio [HR] = 1.64 [CI 1.17–2.29], $p = 0.004$) compared to controls, but varied by contrast-enhancement pattern: Diffusely enhancing C_{MET} had equivalent mortality to controls ($p = 0.21$)

*Correspondence: chana5@mskcc.org; jww2001@med.cornell.edu; weinsaftj@mskcc.org

¹ Department of Medicine, Memorial Sloan Kettering Cancer Center, New York, NY, USA

Full list of author information is available at the end of the article



© The Author(s) 2021. **Open Access** This article is licensed under a Creative Commons Attribution 4.0 International License, which permits use, sharing, adaptation, distribution and reproduction in any medium or format, as long as you give appropriate credit to the original author(s) and the source, provide a link to the Creative Commons licence, and indicate if changes were made. The images or other third party material in this article are included in the article's Creative Commons licence, unless indicated otherwise in a credit line to the material. If material is not included in the article's Creative Commons licence and your intended use is not permitted by statutory regulation or exceeds the permitted use, you will need to obtain permission directly from the copyright holder. To view a copy of this licence, visit <http://creativecommons.org/licenses/by/4.0/>. The Creative Commons Public Domain Dedication waiver (<http://creativecommons.org/publicdomain/zero/1.0/>) applies to the data made available in this article, unless otherwise stated in a credit line to the data.

whereas prognosis was worse with heterogeneous C_{MET} ($p=0.005$) and more strongly predicted by heterogeneous enhancement ($HR=1.97$ [CI 1.23–3.15], $p=0.005$) than lesion size ($HR=1.11$ per 10 cm [CI 0.53–2.33], $p=0.79$).

Conclusions: Contrast-enhancement pattern and location of C_{MET} on CMR impacts prognosis. Embolic events vary by C_{MET} location, with likelihood of PE greatest with right-sided lesions. Heterogeneous enhancement—a marker of tumor avascularity on LGE-CMR—is a novel marker of increased mortality risk.

Keywords: Cardiovascular magnetic resonance, Cardio-oncology, Cardiac neoplasm

Background

Nearly 17 million Americans are living with cancer [1], among whom cardiac metastases (C_{MET}) bear a major impact on therapeutic decision-making and prognosis. Survival has markedly improved for patients with advanced (stage IV) cancer, resulting in a growing population at risk for C_{MET} and its serious consequences. Data from our group and others have shown C_{MET} to be common with advanced cancer, occurring in up to 20% of patients. [2–6] Embolic events—which can occur when lesions dislodge from the heart—are a leading source of morbidity and mortality among patients with C_{MET} . Given that a growing array of new therapies and anticoagulants are available to potentially reduce risk, improved strategies to guide therapy and refine prognostic risk stratification for patients at risk for C_{MET} are of substantial importance.

Cardiovascular magnetic resonance (CMR) has been well-validated for tissue characterization of cardiac masses. [2, 4, 7–12] Whereas neoplasms can vary in morphology, vascular supply is an intrinsic requirement for tumor growth and this property can be leveraged for diagnostic purposes. Using the technique of late gadolinium enhancement (LGE), CMR can identify neoplasms based on vascularity as manifested by presence of contrast-enhancement. [13] It is also known that neoplasms can vary in pattern of contrast enhancement on LGE-CMR, and that some lesions can include enhancing and non-enhancing components. [2–4] Consistent with this, pathology studies have shown that some neoplasms can have avascular foci (“tumor necrosis”)—a finding linked to aggressive tumor growth and adverse outcomes. [14] Impact of tumor avascularity—as manifested by contrast hypo-enhancement on LGE-CMR—has yet to be tested as a prognostic marker among patients with C_{MET} .

This study encompassed a broad cohort of systemic cancer patients with C_{MET} as well as controls (without C_{MET}) matched for cancer etiology and stage. CMR was performed using a tailored protocol to assess presence and pattern of C_{MET} enhancement—including standardized grading and quantitative analyses—as well as standardized assessment of lesion size and mobility. The goal was to test impact of C_{MET} anatomic distribution and

contrast enhancement pattern on embolic events and mortality.

Methods

Study population

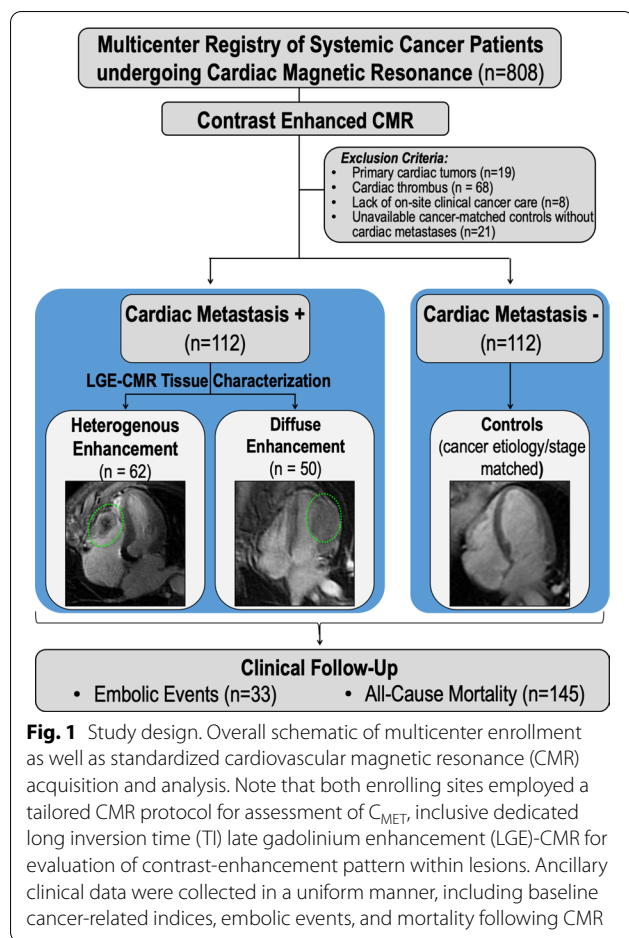
The population was comprised of adults (≥ 18 years) with advanced (stage IV) systemic cancer and C_{MET} , and controls without C_{MET} , matched (1:1) for cancer diagnosis: Presence or absence of C_{MET} was established using the reference of LGE-CMR, on which it was defined via established criteria as a discrete tissue prominence with vascularity as evidenced by contrast-enhancement. [2–4] Subjects with CMR-evidenced intracardiac thrombi were excluded.

Figure 1 provides a schematic of the research protocol. As shown, study participants were accrued at two tertiary care centers with dedicated cancer care programs (Memorial Sloan Kettering Cancer Center [MSKCC], Weill Cornell Medicine—New York Presbyterian Hospital, New York, New York, USA) that share an integrated CMR program. Clinical data were collected in a standardized manner, including cancer diagnosis and stage, anti-cancer and anticoagulant therapies, as well as clinically documented embolic events (pulmonary embolism (PE), cerebrovascular events (CVA), systemic [splenic, peripheral] emboli) within 6 months of CMR. Mortality was assessed to test prognosis in relation to anatomic and tissue characteristics of C_{MET} .

This study entailed analysis of data acquired for clinical purposes between 2012 and 2020; no dedicated interventions were performed for research purposes. Ethics approval for this protocol was provided by the MSKCC and Weill Cornell Medicine institutional review boards, each of which approved a waiver of informed consent for analysis of pre-existing clinical data.

Imaging protocol

CMR was performed on commercial (1.5 T [87%], 3 T [13%]) scanners (General Electric Healthcare, Waukesha, Wisconsin, USA). Exams included electrocardiogram (ECG)-gated cine- and LGE components; both were obtained in contiguous left ventricular (LV) short (mitral annulus—apex) and long axis (2, 3, and 4 chamber) orientations. Cine-CMR utilized a balanced steady-state



free precession (bSSFP) pulse sequence. LGE-CMR utilized an inversion recovery pulse sequence; images were acquired after gadolinium (0.2 mmol/kg) infusion (“long-TI” [600 ms] = 5–10 min, conventional [~300 ms] 10–30 min post contrast). Contrast administration entailed gadoterate meglumine (Dotarem, Guerbet, Villepinte, France) or gadopentetate dimeglumine (Magnevist, Bayer Schering Pharma, Berlin, Germany), which were respectively utilized in 53% and 47% of exams. Conventional and long inversion time (TI) LGE-CMR were used to discern presence and pattern of enhancement in C_{MET} , concordant with prior methods validated by our group and others. [2–4, 9–11] Conventional LGE-CMR was acquired in all patients; additional breath holds for long TI imaging were tolerated in 92% (103/112) of patients with C_{MET} .

Image analysis

C_{MET} was identified on LGE-CMR based on lesion-associated vascularity in accordance with established qualitative (visual) criteria. [2–4] To test modifying impact of C_{MET} tissue properties on cancer associated

outcomes, lesions were further classified into two distinct categories—*diffuse enhancement* (homogenous contrast enhancement throughout lesion) or *heterogeneous enhancement* (enhancing and non-enhancing components within a lesion).

C_{MET} were scored in a binary manner (present/absent), localized based on chamber (right atrium [RA], right ventricle [RV], left atrium [LA], left ventricle [LV]) or pericardial involvement, and classified as intra-cavitary (predominantly localized to cardiac chamber) or intramural (invading into myocardium). Intra-cavitary lesions were further graded for lesion mobility, with highly mobile lesions classified as demonstrating dys-synchronous mobility in relation to adjacent myocardium. Figure 2 provides representative examples of C_{MET} types, including heterogeneous and diffusely enhancing lesions with intra-cavitary or intramyocardial involvement.

Quantitative analyses were used to assess magnitude of contrast enhancement within C_{MET} . Concordant with established methods used by our group, [2, 4] aggregate signal-to-noise ratio (SNR) and contrast-to-noise ratio (CNR) ratios were measured on the long TI LGE-CMR image on which the lesion was most prominent. Intra-cardiac lesion size (area, linear dimensions) was measured on cine-CMR datasets, which were co-localized with LGE-CMR for purpose of analyses. For patients with multiple C_{MET} , the largest lesion was used for quantitative analysis and patient categorization (i.e. heterogeneous or diffusely enhancing). Ancillary analyses included quantification of cardiac chamber size and function, which were measured on cine-CMR using standard planimetry methods. [3]

Prognostic assessment

Electronic medical records were reviewed to assess embolic events (PE, CVA, systemic [i.e. splenic, peripheral] emboli) within 6 months of imaging, as well as all-cause mortality after CMR so as to test clinical events in relation to presence and type of C_{MET} . All-cause mortality and embolic events were ascertained blinded to CMR analyses.

Statistical methods

Comparisons between groups with or without C_{MET} , and between C_{MET} subtypes (heterogeneous, diffusely enhancing) were made using Student’s t-tests (expressed as mean \pm standard deviation) for continuous variables, and Chi-square or Fisher’s exact tests for categorical variables: Paired testing (t-tests or McNemar’s tests) was employed for matched case–control comparisons. Univariate logistic regression was used to test variables associated with mortality and embolic events; variables significantly associated with outcomes in univariate

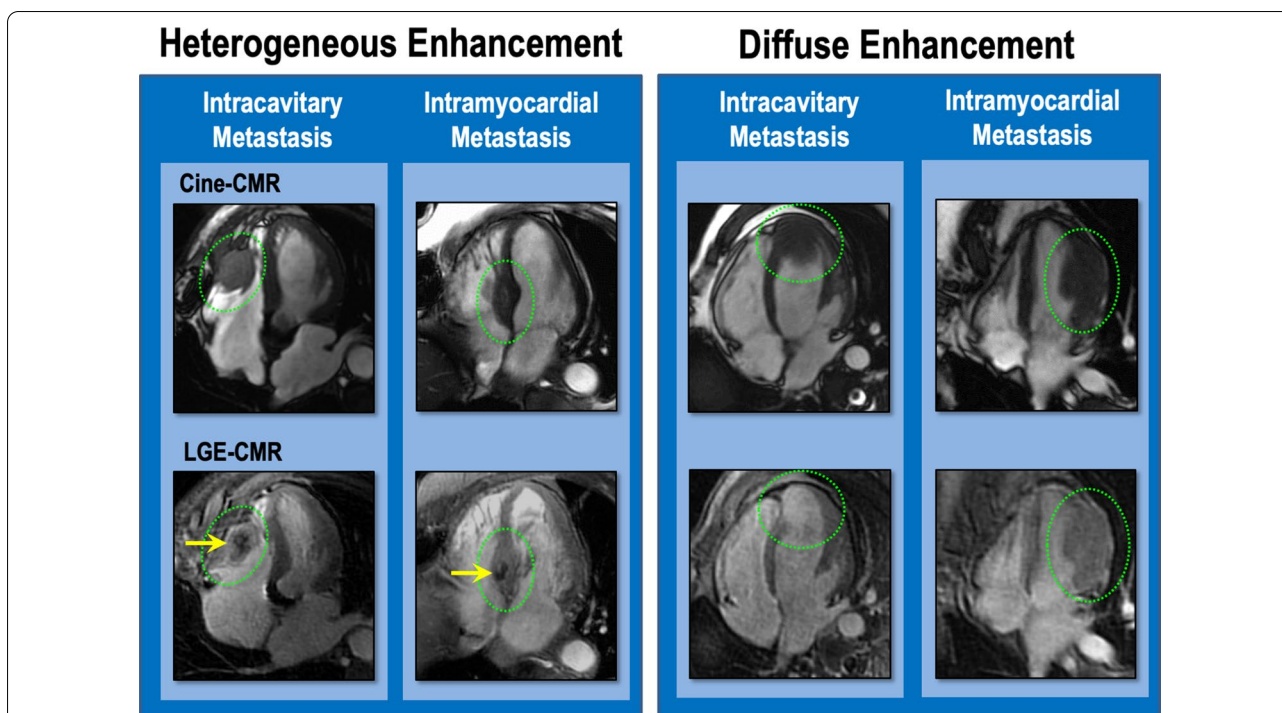


Fig. 2 Representative examples. Representative examples of C_{MET} classifications, including heterogeneously (left) and diffusely (right) enhancing lesions with intracavitary or intramural location [top: cine-CMR | bottom: LGE-CMR]. Lesions denoted by green circles. Note focal hypo-enhancement (yellow arrows) within heterogeneously enhancing lesions, corresponding to C_{MET} avascular components

analysis were then tested together in adjusted models. The Kaplan–Meier method was used to calculate survival; follow-up duration was reported as median with interquartile range (IQR). Cox proportional hazards models compared mortality risk between groups, including prognostic utility of C_{MET} features. Calculations were performed using SPSS (Statistical Package for the Social Sciences, International Business Machines, Inc., Armonk, New York, USA). Two-sided $p < 0.05$ was deemed indicative of statistical significance.

Results

Population characteristics

The population comprised 224 adults with advanced (stage IV) systemic cancer undergoing CMR, including 112 patients with C_{MET} as defined by LGE-CMR, and unaffected (C_{MET}^-) controls matched for primary cancer diagnosis and stage.

Table 1 details population characteristics, together with comparisons between cancer patients with C_{MET} and their respective controls. As shown, cancer diagnosis varied among patients with C_{MET} : Sarcoma, lung, genitourinary, gastrointestinal cancers, and skin/melanoma comprised the leading primary cancer diagnoses, although the population also included patients with primary cancers not typically associated with C_{MET} (e.g.

endocrine, head/neck). Regarding anti-cancer regimen, patients with C_{MET} were more likely to be treated with mediastinal radiation therapy and low molecular weight heparin (both $p = 0.01$) but were otherwise similar with respect to matched controls. Of note, nearly half (49%) of patients with CMR-evidenced C_{MET} had a subsequent change in anti-cancer medication regimen following CMR; 16% received new mediastinal/chest radiation within 3 months after imaging.

Regarding cardiac indices, cancer-matched controls referred for CMR were more likely to have adverse left sided chamber remodeling—as evidenced by lower LV ejection fraction and larger chamber size (both $p < 0.01$), but groups had similar right sided structural and functional indices ($p = NS$).

Cardiac metastasis location in relation to contrast enhancement

Anatomic location of C_{MET} varied (LV 32% | LA 22% | , RV 37% | RA 30% | multi-chamber involvement 30%): Left and right sided chamber involvement were near equal in prevalence (50%, 58% respectively). Regarding C_{MET} tissue properties, 53% of patients had heterogeneously enhancing lesions (enhancing and non-enhancing components on LGE-CMR), whereas 47% had diffusely enhancing lesions without non-enhancing components.

Table 1 Population characteristics

	Overall (n = 224)	C _{MET+} (n = 112)	C _{MET-} Controls (n = 112)	p ^b
Clinical characteristics				
Age (years)	58 ± 17	57 ± 16	58 ± 18	0.68
Gender (male)	59% (133)	63% (71)	55% (62)	0.23
Body surface area (kg/m ²) ^a	1.9 ± 0.3	1.9 ± 0.3	1.9 ± 0.3	0.55
Cancer etiologies ^b				
Sarcoma	20% (44)	20% (22)	20% (22)	–
Lung	16% (36)	16% (18)	16% (18)	–
Genitourinary	15% (34)	15% (17)	15% (17)	–
Gastrointestinal	13% (28)	13% (14)	14% (14)	–
Skin/melanoma	13% (28)	13% (14)	13% (14)	–
Lymphoma	8% (18)	8% (9)	8% (9)	–
Endocrine	8% (18)	8% (9)	8% (9)	–
Anti-cancer regimen				
Chemotherapy				
Alkylating agent	44% (99)	46% (52)	41% (46)	0.47
Plant alkaloid	31% (70)	32% (36)	30% (34)	0.88
Antitumor antibiotics	21% (48)	21% (23)	23% (26)	0.69
Antimetabolites	31% (70)	35% (39)	27% (30)	0.19
Topoisomerase inhibitors	8% (17)	7% (8)	8% (9)	1.00
Anthracycline	21% (46)	19% (21)	23% (26)	0.41
Monoclonal antibodies				
Tyrosine kinase inhibitors	23% (51)	20% (22)	28% (31)	0.21
Other kinase inhibitors	4% (8)	2% (2)	6% (7)	0.18
Immunotherapy	21% (47)	21% (24)	20% (22)	0.84
Radiation therapy				
Mediastinal radiation	13% (28)	18% (20)	7% (8)	0.01
Other radiation	38% (84)	40% (45)	35% (39)	0.49
Anticoagulation therapy				
Overall	22% (50)	28% (31)	17% (19)	0.07
Low molecular weight heparin	24% (53)	32% (36)	16% (18)	0.01
Warfarin	3% (6)	4% (4)	2% (2)	0.69
Direct Oral Anticoagulant	15% (34)	18% (20)	13% (14)	0.26
Cardiovascular disease risk factors				
Hypertension	43% (97)	41% (46)	45% (51)	0.59
Hyperlipidemia	31% (69)	28% (31)	34% (38)	0.35
Diabetes mellitus	14% (31)	11% (12)	17% (19)	0.23
Smoking	38% (79)	31% (35)	39% (44)	0.26
Cardiopulmonary disease				
Coronary artery disease	11% (24)	11% (12)	11% (12)	1.00
Atrial fibrillation/flutter	16% (35)	13% (14)	19% (21)	0.27
Pulmonary disease	6% (13)	3% (3)	9% (10)	0.09
Pulmonary hypertension	16% (36)	13% (14)	20% (22)	0.17
Cardiac morphology and function				
Left ventricle				
Ejection fraction (%)	61 ± 11	63 ± 8	59 ± 12	0.004
End-diastolic volume (mL)	124 ± 41	114 ± 34	131 ± 43	0.002
End-systolic volume (mL)	51 ± 29	42 ± 17	57 ± 32	< 0.001
Stroke volume (mL)	73 ± 21	72 ± 22	75 ± 21	0.38
Myocardial mass (gm)	118 ± 49	117 ± 55	116 ± 37	0.83

Table 1 (continued)

	Overall (n = 224)	C _{MET+} (n = 112)	C _{MET-} Controls (n = 112)	p ^b
Right ventricle				
Ejection fraction (%)	54 ± 9	54 ± 9	53 ± 8	0.30
End-diastolic volume (mL)	135 ± 44	130 ± 37	141 ± 50	0.08
End-systolic volume (mL)	64 ± 29	60 ± 24	69 ± 32	0.03
Stroke volume (mL)	70 ± 23	70 ± 23	72 ± 23	0.44
Atria				
Left atrial area (cm ²)	20 ± 6	19 ± 5	21 ± 7	0.02
Right atrial area (cm ²)	19 ± 6	19 ± 6	19 ± 6	0.98
Pericardial effusion	24% (53)	30% (33)	19% (21)	0.07

Comparisons between cancer patients with late gadolinium enhancement (LGE) CMR-evidenced cardiac metastases and cancer-matched controls

^s Among patients with cardiac metastases, 26% had multiple lesions (median lesion # 2.4 ± 1.0; lesion size: 3.8 ± 2.2 cm)

C_{MET+}, cardiac metastasis; C_{MET-}, no cardiac metastasis

^a Body surface area

^b Additional cancer diagnoses: breast (4%), head/neck (3%), mesothelioma (1%), multiple myeloma with extramedullary involvement (1% [stage IV via Southwest Oncology Group criteria [22]])

Table 2 compares heterogeneously enhancing and diffusely enhancing C_{MET}. As shown, lesions were similar with respect to anatomic distribution, as evidenced by equivalent patterns of chamber involvement and rates of intra-cavitary location (all p = NS). Regarding lesion size, heterogeneously enhancing lesions were larger, based on linear dimensions (p < 0.05). Quantitative analyses were consistent with lesion classification, as evidenced by higher CNR (reflecting greater differences between enhancing and non-enhancing regions) and lower normalized SNR (reflecting impact of non-enhancing lesions on aggregate lesion signal intensity) in heterogeneously enhancing C_{MET} (both p < 0.001 vs. diffusely enhancing C_{MET}).

Embolic events

Embolic events (within 6 months of CMR) were assessed to test if presence of C_{MET} impacted likelihood of clinical events, and whether this was modified by lesion location or tissue characteristics. A total of 33 embolic events occurred in the study population; events occurred at a median interval of 2 weeks from CMR [IQR 0.5, 9.5 weeks]. As shown in Table 3A, embolic events were over twofold more common among patients with C_{MET} as compared to cancer matched controls (21% vs. 8%, p = 0.006), including increased incidence of PE (13% vs. 5%, p = 0.08): Embolic events occurred at a median interval of 2 weeks from CMR [IQR 0.5, 9.4 weeks].

Data shown in Table 3A also demonstrates that C_{MET} location modified likelihood of clinical events: Whereas patients with right sided lesions had a more than threefold increase in PE (20% vs. 6%, p = 0.02), those with left sided lesions had near identical rates of PE compared to

cancer-matched controls (4% vs. 5%). Among patients with left sided lesions, CVA was more common compared to matched controls, although statistical differences between groups was not achieved in context of low clinical event rates (7% vs. 2%, p = 0.38). Sub-group analyses limited to intracavitary C_{MET} demonstrated a stronger association between lesion location and embolic event rates: Among patients with right sided intracavitary C_{MET}, PE occurred in over one fourth of cases—a rate more than fourfold higher than in matched controls (27% vs. 7%, p = 0.01). Two-thirds (8/12; 67%) of patients with right sided intracavitary C_{MET} who developed PE had lesions graded as highly mobile on cine-CMR.

Notably, increased PE rates among patients with right sided C_{MET} occurred despite frequent anticoagulation: Anticoagulant therapies (warfarin or direct oral anticoagulants) were more commonly utilized in patients with right sided C_{MET} as compared to matched controls (33% vs. 15%, p = 0.02), but were equivalent when among C_{MET} patients with left sided involvement and controls (16% vs. 21%, p = 0.63). Of note, 60% of patients with PE were on anticoagulation at the time of their clinical event (64% in C_{MET} vs 50% in controls, p = 0.64).

Regarding impact of C_{MET} tissue characteristics on embolic events, Table 3B demonstrates that rates of PE were similar between patients with heterogeneous and diffusely enhancing lesions (p = NS), as were rates of left sided embolic events. Figure 3 reports PE rates among patients stratified by both lesion location and tissue characteristics: As shown, PE rates were highest among patients with intracavitary right ventricular lesions (p < 0.001 vs. other groups), whereas partitioning based on lesion tissue characteristics did not stratify event risk

Table 2 Anatomic and tissue properties of cardiac metastases

	Heterogeneously enhancing C _{MET+} (n = 59)	Diffusely enhancing C _{MET+} (n = 53)	p
Clinical characteristics			
Cancer etiologies			
Sarcoma	24% (14)	15% (8)	0.25
Lung	15% (9)	17% (9)	0.80
Genitourinary	19% (11)	11% (6)	0.28
Gastrointestinal	14% (8)	11% (6)	0.72
Skin/Melanoma	7% (4)	19% (10)	0.05
Lymphoma	3% (2)	13% (7)	0.08
Endocrine	10% (6)	6% (3)	0.50
Cardiovascular risk factors			
Hypertension	42% (26)	38% (20)	0.50
Hyperlipidemia	27% (16)	28% (15)	0.89
Diabetes mellitus	10% (6)	11% (6)	0.84
Smoking	24% (14)	40% (21)	0.07
Cardiopulmonary disease			
Coronary artery disease	12% (7)	9% (5)	0.68
Atrial fibrillation/flutter	10% (6)	15% (8)	0.43
Pulmonary disease	3% (2)	2% (1)	1.00
Pulmonary hypertension	15% (9)	9% (5)	0.35
Anatomic properties			
Lesion location			
Left ventricle	36% (21)	28% (15)	0.41
Right ventricle	34% (20)	40% (21)	0.53
Left atrium	20% (12)	25% (13)	0.60
Right atrium	24% (14)	38% (20)	0.11
Pericardium	32% (19)	26% (14)	0.50
Left-sided	53% (31)	47% (25)	0.57
Right-sided	49% (29)	68% (36)	0.04
Bilateral	17% (10)	23% (12)	0.45
Multi-chamber	25% (15)	36% (19)	0.23
Intra-cavitary			
Left ventricle	9% (5)	8% (4)	1.00
Right ventricle	22% (13)	25% (13)	0.76
Left atrium	17% (10)	21% (11)	0.61
Right atrium	17% (10)	26% (14)	0.22
Lesion number (1 2 ≥ 3)	78% 19% 3%	70% 19% 11%	0.26
Lesion size			
Area (cm ²)	16.0 ± 20.8	10.1 ± 16.0	0.10
Perimeter (cm)	15.3 ± 11.3	13.3 ± 12.9	0.39
Maximal length (cm)	5.1 ± 3.7	3.7 ± 2.8	0.02
Orthogonal length (cm)	3.0 ± 2.0	2.4 ± 1.8	0.11
Perimeter/min Length	5.0 ± 1.7	7.3 ± 8.8	0.06
Pericardial effusion	37% (22)	21% (11)	0.06
Tissue properties			
Contrast-to-noise ratio (CNR)	20.5 ± 15.0	7.4 ± 9.1	< 0.001
Signal-to-noise ratio (SNR)	33.1 ± 20.1	44.5 ± 41.2	0.08
Blood pool normalized	0.6 ± 0.2	0.8 ± 0.3	< 0.001

Table 3 Embolic events

A	C _{MET+}	C _{MET-}	p [†]
Overall			
All embolic events	21% (24)	8% (9)	0.006
Pulmonary embolism*	13% (14)	5% (6)	0.08
CVA [†]	8% (9)	4% (4)	0.23
Peripheral embolism	5% (5)	0% (-)	-
Right-sided involvement (n = 65)			
All embolic events	31% (20)	8% (5)	0.001
Pulmonary embolism	20% (13)	6% (4)	0.02
CVA	9% (6)	3% (2)	0.22
Peripheral embolism	8% (5)	0% (-)	-
Left-sided involvement (n = 56)			
All embolism	13% (7)	7% (4)	0.55
Pulmonary embolism	4% (2)	5% (3)	1.00
CVA	7% (4)	2% (1)	0.38
Peripheral embolism	2% (1)	0% (-)	-
Intra-cavitary metastasis			
Right-sided Involvement (n = 45)			
All embolic events	36% (16)	9% (4)	0.002
Pulmonary embolism	27% (12)	7% (3)	0.01
CVA	11% (5)	4% (2)	0.38
Peripheral embolism	7% (3)	0% (-)	-
Left-sided Involvement (n = 31)			
All embolic events	29% (9)	10% (3)	0.15
Pulmonary embolism	16% (5)	7% (2)	0.45
CVA	13% (4)	3% (1)	0.38
Peripheral embolism	3% (1)	0% (-)	-
B	Heterogeneous enhancement C _{MET+} (n = 59)	Diffuse enhancement C _{MET+} (n = 53)	P
All embolic events	24% (14)	19% (10)	0.53
Pulmonary embolism	15% (9)	9% (5)	0.35
CVA	10% (6)	6% (3)	0.50
Peripheral embolism	2% (1)	8% (4)	0.19

* Pulmonary embolism

† Cerebrovascular events

($p = NS$). **Table 4** demonstrates that increased PE risk among patients with right ventricular C_{MET} was accompanied by impaired RV function, as evidenced by lower absolute RV ejection fraction (RVEF) and higher prevalence of RV dysfunction (both $p < 0.05$). Of note, among patients with RV C_{MET}, RVEF was similar between those who had PE prior to, compared to those who had PE after CMR ($51.0 \pm 12.7\%$ vs $53.5 \pm 3.8\%$, $p = 0.72$)—consistent with the notion that event driven changes in RV systolic function were not responsible for observed associations between impaired RV function and PE. Data shown in Additional file 1: Table S1 tests both clinical and CMR parameters in relation to PE. As shown, both gastrointestinal cancer etiology and right sided C_{MET} were each

associated with increased likelihood of PE in univariate regression analysis, and each parameter remained associated with PE ($p < 0.01$) when the two parameters (gastrointestinal cancer etiology, right sided intracavitary C_{MET}) were tested together in an adjusted model.

Mortality

Follow-up was performed for a median duration of 0.8 years [IQR 0.3–1.67], during which a total of 145 deaths occurred. Figure 4 provides Kaplan Meier survival curves for the overall cohort of C_{MET} patients and cancer-matched controls, as well as for subgroups based on C_{MET} tissue characteristics. As shown (a), mortality

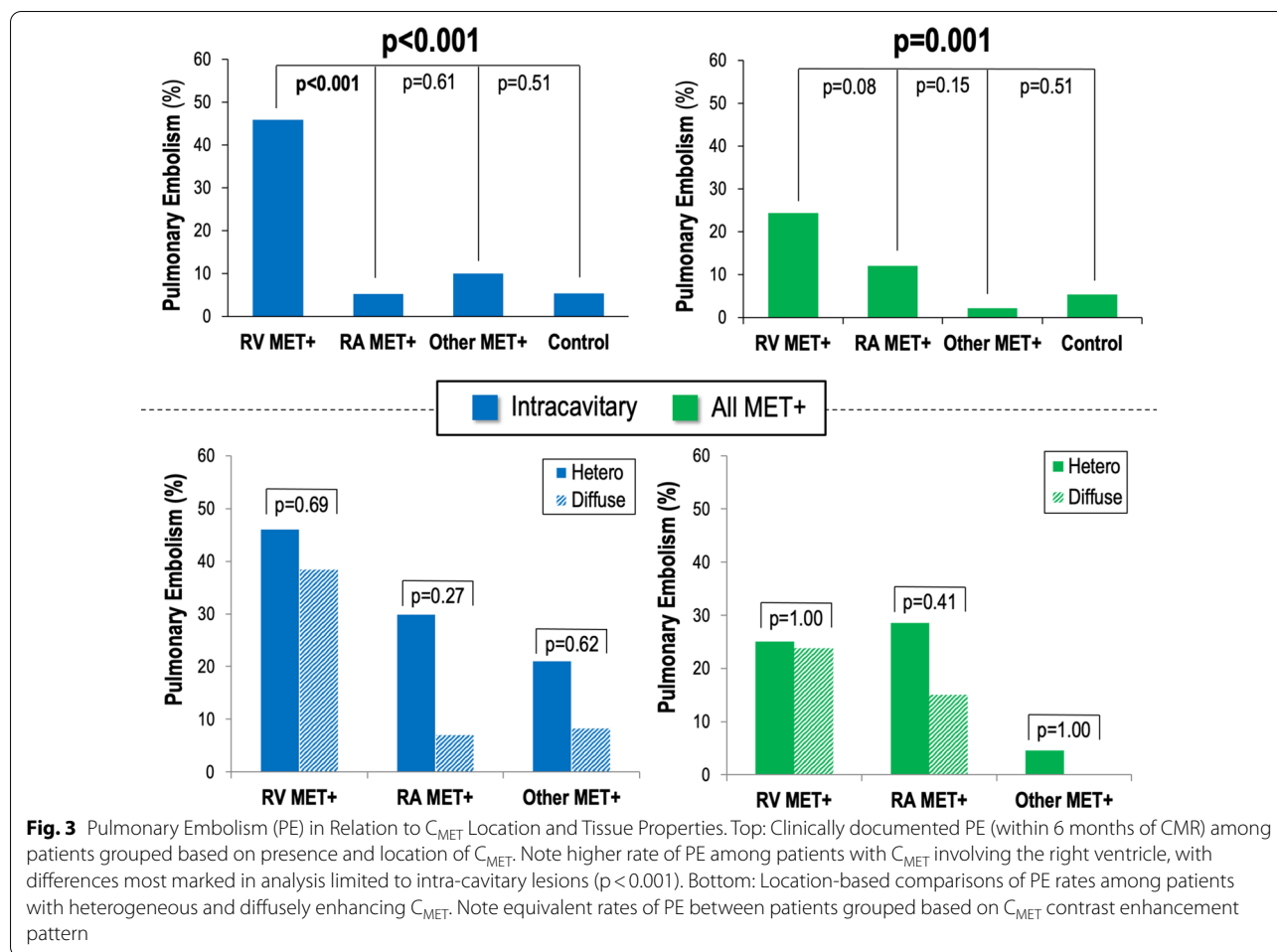


Fig. 3 Pulmonary Embolism (PE) in Relation to C_{MET} Location and Tissue Properties. Top: Clinically documented PE (within 6 months of CMR) among patients grouped based on presence and location of C_{MET}. Note higher rate of PE among patients with C_{MET} involving the right ventricle, with differences most marked in analysis limited to intra-cavitary lesions ($p < 0.001$). Bottom: Location-based comparisons of PE rates among patients with heterogeneously and diffusely enhancing C_{MET}. Note equivalent rates of PE between patients grouped based on C_{MET} contrast enhancement pattern

risk was higher among C_{MET} patients compared to controls (HR = 1.64 [CI 1.17–2.29], $p = 0.004$): Median survival after CMR was shorter among patients with C_{MET} (9.7 months [IQR 4.0–21.7] vs. 15.1 months [5.4–60.3], $p = 0.004$), paralleled by increased 6-month (39% vs. 28%, $p = 0.12$) and 1 year (57% vs. 46%, $p = 0.2$) mortality.

Figure 4b demonstrates that mortality differed in relation to tissue characteristics of C_{MET}: Whereas patients with diffusely enhancing C_{MET} had near equivalent mortality to matched controls ($p = 0.21$), prognosis was worse among patients with heterogeneously enhancing C_{MET} ($p = 0.005$)—including increased 6-month (44% vs. 26%) and 1 year (65% vs. 41%) mortality in respective case-control comparisons (both $p < 0.05$). As shown in Table 5, heterogeneously enhancing C_{MET} conferred higher risk for mortality (HR 1.97 [CI 1.23–3.15], $p = 0.005$) than did number of lesions (HR 1.67 [CI 1.31–2.12], $p < 0.001$) or lesion size (1.11 per 10 cm [CI 0.53–2.33], $p = 0.79$). Additionally, whereas lymphoma was the sole cancer diagnosis associated with differential (improved) prognosis, an adjusted model analysis inclusive of this

variable together with LGE-CMR tissue characterization data demonstrated heterogeneously enhancing C_{MET} to remain associated with increased mortality (1.97 [CI 1.23–3.16], $p = 0.005$).

Discussion

To our knowledge, this is the first study to test LGE-CMR pattern of C_{MET} as a prognostic marker in patients with systemic cancer, with focus on localized hypo-enhancement (a marker of tumor avascularity) as a novel marker of adverse prognosis. Results add to a growing body of literature by our group and others validating LGE-CMR in relation to histopathology and demonstrating clinical utility of this approach to guide diagnostic, prognostic, and therapeutic decision-making for patients with known or suspected cardiac masses. Key findings are as follows: First, among a broad cohort of advanced cancer patients, C_{MET} contrast-enhancement pattern varied—prevalence of diffusely (47%) and heterogeneously enhancing (53%) lesions was near equivalent. Quantitative analyses demonstrated heterogeneously enhancing C_{MET} to have

Table 4 Cardiac remodeling in patients with and without right ventricular cardiac metastases

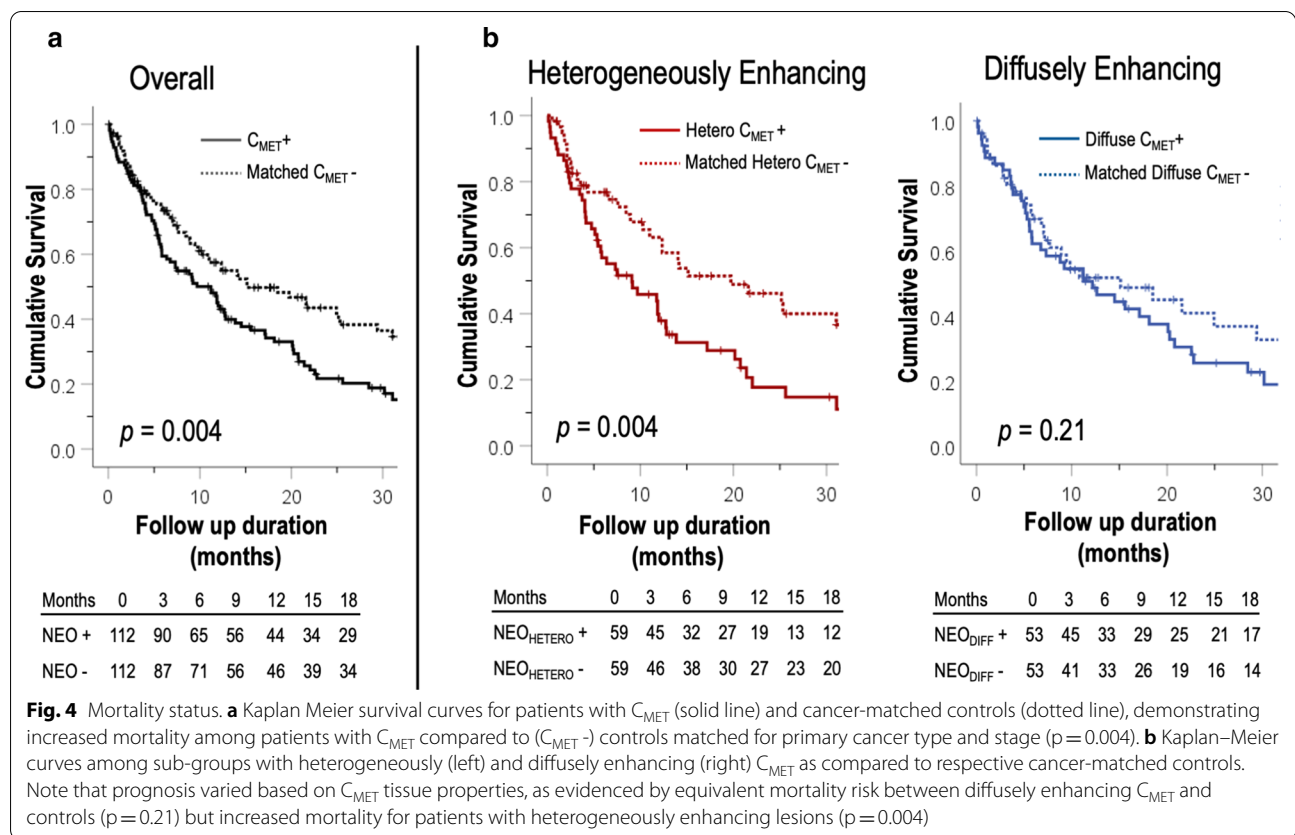
	Right ventricular C _{MET+} (n = 41)	Other C _{MET+} (n = 71)*	p
Cardiac morphology			
Left ventricle			
Ejection fraction (%)	62 ± 8	64 ± 9	0.27
Ejection fraction (< 50%)	10% (4)	9% (6)	1.00
End-diastolic volume (mL)	110 ± 33	117 ± 35	0.27
End-systolic volume (mL)	42 ± 17	42 ± 17	0.83
Stroke volume (mL)	68 ± 21	75 ± 23	0.12
Myocardial mass (gm)	130 ± 81	112 ± 37	0.19
Right ventricle			
Ejection fraction (%)	52 ± 11	56 ± 8	0.048
Ejection fraction (< 50%)	34% (14)	16% (11)	0.03
End-diastolic volume (mL)	133 ± 41	129 ± 36	0.60
End-systolic volume (mL)	65 ± 30	57 ± 20	0.11
Stroke volume (mL)	68 ± 23	71 ± 23	0.54
Atria			
Left atrial area (cm ²)	18.2 ± 5.7	19.5 ± 5.1	0.25
Right atrial area (cm ²)	19.8 ± 6.7	18.7 ± 5.0	0.36
Lesion characteristics			
Anatomic properties			
Area (cm ²)	9.5 ± 12.4	13.3 ± 19.7	0.27
Perimeter (cm)	14.3 ± 14.0	13.6 ± 10.5	0.79
Maximal Length (cm)	4.1 ± 2.7	4.6 ± 3.9	0.43
Orthogonal Length (cm)	2.3 ± 1.5	2.9 ± 2.2	0.09
Perimeter/Min Length	7.2 ± 8.3	5.6 ± 4.7	0.18
Tissue properties			
Heterogenous Enhancement	49% (20)	55% (39)	0.53
Contrast to Noise Ratio (CNR)	13.5 ± 14.8	14.8 ± 13.8	0.64
Signal-to-Noise Ratio (SNR)	46.8 ± 46.9	33.5 ± 17.0	0.10
Blood pool normalized	0.7 ± 0.3	0.6 ± 0.3	0.007

* Inclusive of left ventricular, left atrial, and right atrial cardiac metastases

more aggressive features, as evidenced by larger lesion size and lower SNR (as would be expected in context of tumor avascularity). Second, presence and distribution of C_{MET} impacted likelihood of embolic events. Aggregate embolic events were higher among patients with C_{MET} compared to cancer matched controls (21% vs. 8%, $p=0.006$), C_{MET} location modified likelihood of events: Whereas patients with right sided lesions had a threefold increase in PE (20% vs. 6%, $p=0.02$), those with left sided lesions had near identical event rates to those of (C_{MET} -) controls (4% vs. 5% $p=1.00$). Embolic event rates did not vary in relation to C_{MET} by tissue properties, as evidenced by equivalent rates of PE among patients with diffuse and heterogeneously enhancing right ventricular lesions. Third, mortality risk conferred by C_{MET} varied in relation to contrast-enhancement pattern. During a median follow-up of 0.7 years [IQR 0.3–1.7], patients with and without diffusely enhancing C_{MET} had equivalent mortality to controls ($p=0.21$), whereas prognosis

was worse among patients with heterogeneously enhancing C_{MET} compared to controls matched for cancer etiology and stage ($p=0.005$).

Our finding that heterogeneous lesion enhancement constitutes an adverse prognostic marker among patients with C_{MET} is consistent with established concepts in tumor biology: Tumor necrosis—as would be expected to result in avascularity and thus impaired contrast uptake—is a known marker of aggressive phenotype: Uncontrolled oncogene driven proliferation of neoplastic cells exhausts oxygen supply from normal vasculature, resulting in localized hypoxia which upregulates production of angiogenic factors and triggers neovascularization. [15, 16] However, vessels formed in response to hypoxia lack normal physiological angiogenesis—providing a nidus for chaotic tumor architecture and vascular leakiness. Hypoxia alters cancer metabolism to foster survival during stress and drive malignant progression, resulting in resistance to anti-cancer



therapy and accelerated tumor growth. Consistent with this, magnetic resonance imaging (MRI) studies focused on extra-cardiac areas—including neurologic and renal cancers—have associated contrast hypo-enhancement (tumor necrosis) with chemotherapeutic resistance and increased mortality. [14, 17, 18].

Regarding embolic events, our data demonstrated C_{MET} location to be strongly associated with outcomes—as evidenced by increased rates of PE among patients with RV intracavitary C_{MET} . Our finding that embolic events were equivalent between patients with diffuse and heterogeneous C_{MET} is not unexpected, given that avascular components were typically centrally located within lesions and would thus be unexpected to provide a nidus for embolization. Regarding mechanism, our data demonstrated patients with RV C_{MET} to have lower RV systolic function than those with C_{MET} in other locations ($p < 0.05$)—possibly due to mechanical tumor effects or treatment related (i.e. radiation-induced) cardiac injury. Based on this, it is possible that localized stasis could contribute to development of super-imposed thrombosis on neoplastic lesions—providing a nidus for embolic events. Whereas heterogeneous enhancement (as would be expected in context of tumor with superimposed thrombus) was not identified as a risk factor for embolic events, it is possible

that micro-thrombi developed prior to or following the time of CMR, or that spatial resolution of LGE-CMR was insufficient for diagnostic detection. It is also possible that emboli stemmed from tumor dislodgement rather than primary thrombotic processes or from insufficient anticoagulation—concepts supported by the fact that nearly two-thirds (63%) of C_{MET} patients were on anticoagulation at the time of clinical events, as well as recent data showing high embolic event rates in non-cancer [10, 19] and cancer populations [20] with cardiac thrombus treated with anticoagulants. Future research, including imaging using high resolution 3D LGE-CMR [21] and prospective trials testing relative efficacy of anticoagulant regimens or targeted resection in cancer patients with C_{MET} , are necessary to further test these concepts.

Limitations

Several limitations should be noted. First, whereas our study encompassed a broad cohort of cancer patients undergoing CMR and clinical follow-up at two institutions, it should be recognized that embolic events were ascertained based on clinical documentation and/or diagnostic testing. In this context, it is likely that subtle clinical events were under-reported, or that clinical considerations may have influenced testing such that embolic

Table 5 Mortality predictors

	Hazard ratios	p
Clinical characteristics		
Age (years)	1.00 [CI 1.00–1.01]	0.36
Gender (male)	1.25 [CI 0.88–1.76]	0.20
Cancer etiologies		
Sarcoma	0.91 [CI 0.61–1.37]	0.65
Lung	1.45 [CI 0.95–2.21]	0.08
Genitourinary	1.12 [CI 0.73–1.73]	0.59
Gastrointestinal	1.56 [CI 0.96–2.54]	0.07
Skin/melanoma	0.71 [CI 0.41–1.20]	0.20
Lymphoma	0.40 [CI 0.19–0.86]	0.02
Endocrine	0.62 [CI 0.31–1.22]	0.16
Cardiovascular risk factors		
Hypertension	0.98 [CI 0.70–1.35]	0.86
Hyperlipidemia	1.00 [CI 0.70–1.44]	0.99
Diabetes mellitus	0.87 [CI 0.52–1.46]	0.59
Smoking	1.01 [CI 0.71–1.41]	0.98
Cardiopulmonary disease		
Coronary artery disease	1.36 [CI 0.84–2.21]	0.21
Atrial fibrillation/flutter	1.16 [CI 0.74–1.82]	0.52
Pulmonary disease	0.86 [CI 0.41–1.77]	0.67
Pulmonary hypertension	1.33 [CI 0.86–2.06]	0.20
Cardiac morphology		
Left ventricle		
Ejection fraction	1.01 [CI 0.99–1.03]	0.21
Ejection fraction (< 50%)	0.82 [CI 0.50–1.36]	0.44
End-diastolic volume	1.00 [CI 0.99–1.00]	0.06
End-systolic volume	0.99 [CI 0.99–1.00]	0.07
Right ventricle		
Ejection fraction	1.02 [CI 1.00–1.04]	0.09
Ejection fraction (< 50%)	0.84 [CI 0.57–1.26]	0.40
C_{MET} Lesion Characteristics		
C_{MET} (presence vs. absence)*	1.64 [CI 1.17–2.29]	0.004
Anatomic properties		
Lesion number	1.67 [CI 1.31–2.12]	< 0.001
Multiple lesions	1.94 [CI 1.23–3.06]	0.004
Lesion size (maximal diameter [per 10 cm])	1.11 [CI 0.53–2.33]	0.79
Lesion size (area [per 10 cm ²])	0.99 [CI 0.85–1.15]	0.88
Intra-cavitary lesion	1.27 [CI 0.81–1.97]	0.30
Tissue properties*		
Heterogeneous enhancement	1.97 [CI 1.23–3.15]	0.005
Diffuse enhancement	1.36 [CI 0.84–2.21]	0.21
Adjusted multivariate model†		
Lymphoma (cancer etiology)	0.44 [CI 0.11–1.79]	0.24
Heterogeneous enhancement	1.97 [CI 1.23–3.16]	0.005

* Comparison between cancer patients with CMR-evidenced cardiac metastases and cancer-matched controls

† Regression analysis performed incorporating lymphoma (sole cancer associated with differential [improved] prognosis) and C_{MET} heterogeneous enhancement together in an adjusted model (no additional variables included in adjusted models)

events such as stroke were under-diagnosed. It should be noted that our study was unable to reliably ascertain all potential cancer related clinical indices or derive aggregate classifications of disease chronicity and performance status. Thus, while our results demonstrate that location and contrast-enhancement pattern of LGE-CMR evidenced C_{MET} impacts clinical outcomes, further research is warranted to test whether associations observed in the current study are modified by cancer etiology, treatment type, and/or overall health status. Second, whereas our study utilized LGE-CMR for tissue characterization of C_{MET} , alternative approaches to assess vascularity such as quantitative LGE thresholds, perfusion, parametric mapping, or susceptibility weighted CMR were not tested. Whereas current findings demonstrate heterogeneous contrast uptake pattern within C_{MET} to be a marker of increased mortality risk, knowledge gaps persist as to the relative utility of different imaging approaches to assess tumor necrosis or additional tissue properties such as hemorrhage and calcification. It is also important to recognize that whereas prior studies have validated LGE-CMR tissue characterization of masses in relation to pathology and other standards including metabolic imaging and outcomes, [3, 4, 10] lack of systematic biopsy sampling in the current cohort (for whom invasive cardiac tissue sampling was uncommon in context of advanced cancer) prohibited direct comparison of LGE-CMR enhancement pattern to pathology findings. An additional limitation relates to the relatively small number of embolic events (n=33) in this study, which may explain the wide confidence intervals with respect to observed associations of C_{MET} and GI cancer etiology with PE: In this context, current results should be considered more exploratory than definitive, thus highlighting the need to test them further in larger scale studies. Future research is also warranted to test whether alternative protocols using low dose contrast administration or non-contrast approaches (e.g. T1 mapping) provide equivalent diagnostic and prognostic utility in cancer patients with known or suspected C_{MET} .

Conclusions

Location and contrast-enhancement pattern of C_{MET} impact clinical outcomes, with RV lesion location associated with PE and heterogeneous enhancement conferring increased mortality. Given current findings, future research is warranted to test anticoagulant strategies in cancer populations, whether adverse prognosis conferred by heterogeneous lesion enhancement stems from accelerated tumor growth, and whether tailored therapies—paired to lesion tissue characteristics—improves clinical outcomes for cancer patients with C_{MET} .

Abbreviations

bSSFP: Balanced steady-state free precession; CI: Confidence interval; C_{MET} : Cardiac metastasis; CMR: Cardiovascular magnetic resonance; CNR: Contrast-to-noise ratio; CVA: Cerebrovascular events; ECG: Electrocardiogram; HR: Hazard ratio; IQR: Interquartile range; LA: Left atrium/left atrial; LGE: Late gadolinium enhancement; LV: Left ventricle/left ventricular; MRI: Magnetic resonance imaging; PE: Pulmonary embolism; RA: Right atrium/right atrial; RV: Right ventricle/right ventricular; RVEF: Right ventricular ejection fraction; SNR: Signal-to-noise ratio; TI: Inversion time.

Supplementary Information

The online version contains supplementary material available at <https://doi.org/10.1186/s12968-021-00727-2>.

Additional file 1: Supplementary Table 1.

Acknowledgements

None.

Authors' contributions

Author contributions are as follows: conception and study design (ATC, JWW), data collection and protocol design (ATC, WD, JWW), data analysis and interpretation (ATC, WD, JK, CAK, AP, RS, RPJ, JWW), drafting (ATC, JWW) and revising (MSG, WD, JL, RJ, RS) of the paper. All authors read and approved the final manuscript.

Funding

Memorial Sloan Kettering Cancer Center Support Grant/Core Grant P30 CA008748, American Heart Association 18CDA34080090 (ATC), NIH K23HL140092 (JK), R01HL128278 (JWW).

Availability of data and materials

Study data can be made available to other researchers for purposes of reproducing the results of this study on request (contingent on approval of the Memorial Sloan Kettering Cancer Center and Weill Cornell institutional review boards and assurance of data de-identification).

Ethics approval and consent to participate

This study entailed analysis of data acquired for clinical purposes between 2012 and 2020; no dedicated interventions were performed for research purposes. Ethics approval for this protocol was provided by the Memorial Sloan Kettering Cancer Center and Weill Cornell Medicine institutional review boards, each of which approved a waiver of informed consent for analysis of pre-existing clinical data.

Consent for publication

Not applicable.

Competing interests

The authors disclose no relevant competing interests relevant to this research.

Author details

¹ Department of Medicine, Memorial Sloan Kettering Cancer Center, New York, NY, USA. ² Department of Radiology, Memorial Sloan Kettering Cancer Center, New York, NY, USA. ³ Department of Pharmacological Sciences, Icahn School of Medicine At Mount Sinai, New York, NY, USA. ⁴ Department of Medicine, Weill Cornell Medical College, New York, NY, USA. ⁵ Duke Cardiovascular Magnetic Resonance Center, Durham, NC, USA.

Received: 21 August 2020 Accepted: 3 February 2021

Published online: 05 April 2021

References

1. National Cancer Institute: Surveillance, Epidemiology, and End Results Program. <https://seer.cancer.gov/statistics/>. 2019. Accessed 15 Jan 2020.

- Chan AT, Plodkowski AJ, Pun SC, et al. Prognostic utility of differential tissue characterization of cardiac neoplasm and thrombus via late gadolinium enhancement cardiovascular magnetic resonance among patients with advanced systemic cancer. *J Cardiovasc Magn Reson*. 2017;19:76.
- Chan AT, Fox J, Perez Johnston R, et al. Late gadolinium enhancement cardiac magnetic resonance tissue characterization for cancer-associated cardiac masses: metabolic and prognostic manifestations in relation to whole-body positron emission tomography. *J Am Heart Assoc*. 2019;8:e011709.
- Pun SC, Plodkowski A, Matasar MJ, et al. Pattern and prognostic implications of cardiac metastases among patients with advanced systemic cancer assessed with cardiac magnetic resonance imaging. *J Am Heart Assoc*. 2016;5:9.
- Lam KY, Dickens P, Chan AC. Tumors of the heart. A 20-year experience with a review of 12,485 consecutive autopsies. *Arch Pathol Lab Med*. 1993;117:1027–31.
- Verso M, Agnelli G. Venous thromboembolism associated with long-term use of central venous catheters in cancer patients. *J Clin Oncol*. 2003;21:3665–75.
- Fussen S, De Boeck BWL, Zellweger MJ, et al. Cardiovascular magnetic resonance imaging for diagnosis and clinical management of suspected cardiac masses and tumours. *Eur Heart J*. 2011;32:1551–60.
- Srichai MB, Junor C, Rodriguez LL, et al. Clinical, imaging, and pathological characteristics of left ventricular thrombus: a comparison of contrast-enhanced magnetic resonance imaging, transthoracic echocardiography, and transesophageal echocardiography with surgical or pathological validation. *Am Heart J*. 2006;152:75–84.
- Weinsaft JW, Kim HW, Crowley AL, et al. LV thrombus detection by routine echocardiography: insights into performance characteristics using delayed enhancement CMR. *JACC Cardiovasc Imaging*. 2011;4:702–12.
- Weinsaft JW, Kim HW, Shah DJ, et al. Detection of left ventricular thrombus by delayed-enhancement cardiovascular magnetic resonance prevalence and markers in patients with systolic dysfunction. *J Am Coll Cardiol*. 2008;52:148–57.
- Weinsaft JW, Kim RJ, Ross M, et al. Contrast-enhanced anatomic imaging as compared to contrast-enhanced tissue characterization for detection of left ventricular thrombus. *JACC Cardiovasc Imaging*. 2009;2:969–79.
- Mousavi N, Cheezum MK, Aghayev A, et al. Assessment of cardiac masses by cardiac magnetic resonance imaging: histological correlation and clinical outcomes. *J Am Heart Assoc*. 2019;8:e007829.
- Pazos-Lopez P, Pozo E, Siqueira ME, et al. Value of CMR for the differential diagnosis of cardiac masses. *JACC Cardiovasc Imaging*. 2014;7:896–905.
- Beddy P, Genega EM, Ngo L, et al. Tumor necrosis on magnetic resonance imaging correlates with aggressive histology and disease progression in clear cell renal cell carcinoma. *Clin Genitourinary Cancer*. 2014;12:55–62.
- Bergers G, Benjamin LE. Tumorigenesis and the angiogenic switch. *Nat Rev Cancer*. 2003;3:401–10.
- Eales KL, Hollinshead KE, Tennant DA. Hypoxia and metabolic adaptation of cancer cells. *Oncogenesis*. 2016;5:e190.
- Hammoud MA, Sawaya R, Shi W, Thall PF, Leeds NE. Prognostic significance of preoperative MRI scans in glioblastoma multiforme. *J Neurooncol*. 1996;27:65–73.
- Nowosielski M, Gorlia T, Bromberg JEC, et al. Imaging necrosis during treatment is associated with worse survival in EORTC 26101 study. *Neurology*. 2019;92:e2754.
- Lattuca B, Bouziri N, Kerneis M, et al. Antithrombotic therapy for patients with left ventricular mural thrombus. *J Am Coll Cardiol*. 2020;75:1676–85.
- Plodkowski AJ, Chan A, Gupta D, et al. Diagnostic utility and clinical implication of late gadolinium enhancement cardiac magnetic resonance for detection of catheter associated right atrial thrombus. *Clin Imaging*. 2020;62:17–22.
- Nguyen TD, Spincemaille P, Weinsaft JW, et al. A fast navigator-gated 3D sequence for delayed enhancement MRI of the myocardium: comparison with breathhold 2D imaging. *J Magn Reson Imaging*. 2008;27:802–8.
- Choi J-H, Yoon J-H, Yang S-K. Clinical value of new staging systems for multiple myeloma. *Cancer Res Treat*. 2007;39:171–4.

Publisher's Note

Springer Nature remains neutral with regard to jurisdictional claims in published maps and institutional affiliations.